Inverse Problems **24** (2008) 015008 (13pp) doi:10.1088/0266-5611/24/1/015008

A single-view imaging strategy for transient scattered fields

Ilaria Catapano[1], **Kamal Belkebir**[2] **and Jean-Michel Geffrin**[2]

[1] Istituto per il Rilevamento Elettromagnetico dell' Ambiente, Consiglio Nazionale delle Ricerche (IREA-CNR), I-80124, Napoli, Italy
[2] Institut Fresnel, UMR-CNRS 6133, Université de Provence, Campus de Saint Jérôme, case 162, 13397 Marseille Cedex 20, France

E-mail: catapano.i@irea.cnr.it., kamal.belkebir@fresnel.fr and jean-michel.geffrin@fresnel.fr.

Received 8 July 2007
Published 9 January 2008
Online at stacks.iop.org/IP/24/015008

Abstract

This paper deals with an approach to provide non-invasive characterization of inhomogeneous targets from knowledge of a transient scattered field. This last one is measured by using only one source, which radiates a Gaussian incident pulse. The problem is addressed in the frequency domain rather than directly in the time domain and the reconstruction capabilities of the proposed strategy are verified against experimental data. The experimental setup provides stepped-frequency data measured on a large spectrum support, with a small frequency step. Therefore, it is possible to synthesize pulses with different shapes. This allowed us to test the performance of the proposed inversion strategy. The presented results show that the reconstruction procedure takes advantage of the large spectrum of the incident pulse.

(Some figures in this article are in colour only in the electronic version)

1. Introduction

The use of electromagnetic waves to retrieve the properties of an otherwise inaccessible object is of interest in many applicative contexts wherein non-invasive and non-destructive investigations are required, such as for instance geophysical and geological probing [1], monitoring of subsurface services and so on [2, 3]. However, the imaging of unknown objects from knowledge of their scattered field is not a straightforward task. As a matter of fact, due to the analytical properties of the kernel of the scattering operators [4], an ill-posed problem has to be solved [5]. In addition, due to multiple scattering effects [4], the solution of the inverse scattering problem is further complicated by the nonlinearity of the relationship between data (i.e. scattered fields) and unknowns (permittivity and/or conductivity distributions). As a consequence, during the years, considerable efforts have been put into the derivation of robust

nonlinear optimization schemes and several approaches have been proposed. A review of the most effective strategies is given in [6, 7], where their reconstruction capabilities have also been tested against experimental data. Generally speaking, in the commonly used strategies, the inverse scattering problem is cast as an optimization problem wherein parameters of interest are iteratively built up by minimizing a properly defined cost functional, which is a nonlinear function of unknowns. Since one has to deal (but for some special cases) with a very large number of unknown parameters, the use of global optimization strategies is not usually viable because of the large computational burden. Hence, one has to rely on 'local' techniques, which strongly depend on the initialization and can therefore be trapped into a local minima of the (nonlinear) cost functional, i.e. into a false solution of the problem. Several strategies using a'manageable' degree of nonlinearity have been developed, among which the quadratic model [8] and the modified gradient approaches [9, 10] are worth mentioning. These strategies require a multi-view–multistatic measurement configuration, i.e. data collected by several receivers, which measure the field scattered by the system under test when a large number of source points are used. However, the quality of the reconstruction usually deteriorates when only a reduced amount of illumination views of the investigated domain is available. In this paper, we propose an inversion procedure to retrieve the unknown permittivity profile from the measured scattered transient field when only one electromagnetic source is used. Such a source radiates a Gaussian incident pulse, whose time duration as well as the central frequency of its spectrum can be properly chosen. This kind of source is commonly used in the synthetic aperture radar system for subsurface monitoring [11]. By taking into account the Parseval theorem, the inverse scattering problem is formulated in the frequency domain rather than directly in the time domain and it is solved by means of an inversion procedure, which belongs to the class of the modified gradient methods [9, 10, 12]. In particular, we adopted the approach described in [13, 14] and referred to therein as the modified^2 gradient method (M^2 CG) or a hybrid method. A proof of the effectiveness of the inversion procedure is provided by processing experimental data. In particular, we show how the achievable performances may depend on the incident pulse shape and that the accuracy of the final result may be improved by using a wide-band pulse. This paper is organized as follows. The reference geometry, the adopted notations and the electric field integral equations (EFIE) are given in section 2. Therefore, a definition of the inverse scattering problem and a brief description of the adopted iterative imaging strategy are provided in section 3. In this last one, the method adopted to define the initial guess of the minimization scheme is also explained. Section 4 aims at describing both the experimental setup and the considered targets used to collect the data. Since the use of a large number of receivers and a very narrow frequency step, increases the measurement time without actually increasing the amount of available information, section 5 provides some considerations on the number of receivers and frequencies, which are really necessary to collect independent data. Finally, the results provided by the inversion procedure are presented in section 6. Conclusions follow.

2. Statement of the problem

Consider the reference scenario sketched in figure 1, wherein Ω denotes the investigated domain and Γ the measurement curve. Two-dimensional targets of arbitrary cross section are embedded into a homogeneous medium whose electromagnetic constants are ε_0 and μ_0 (ε_0 and μ_0 being the permittivity and permeability of the vacuum, respectively). The considered materials are assumed to be non-magnetic ($\mu = \mu_0$) and following an Ohmic dispersion model. Therefore, the objects are characterized by a complex permittivity $\varepsilon_c(\mathbf{r}) = \varepsilon(\mathbf{r}) - \mathrm{i}\sigma(\mathbf{r})/\omega$ ($\varepsilon(\mathbf{r})$ and $\sigma(\mathbf{r})$ being the permittivity and the electrical conductivity, respectively, at the position $\mathbf{r}$).

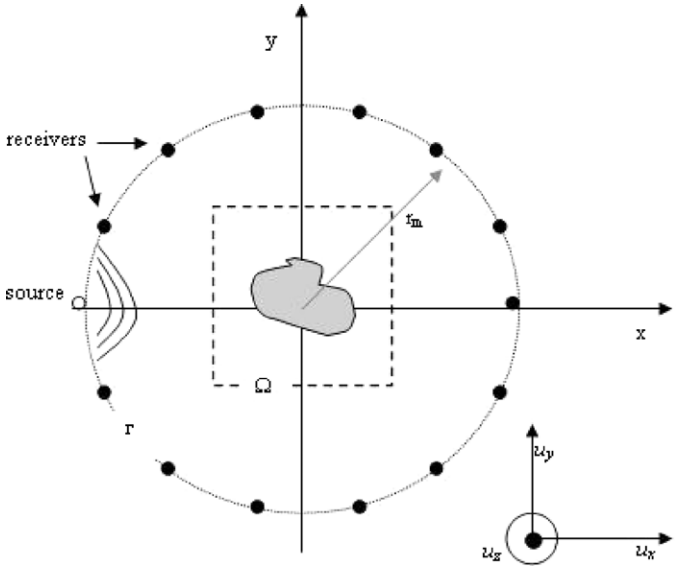

Figure 1. Geometry of the problem.

A right-handed coordinate frame $(O, \mathbf{u}_x, \mathbf{u}_y, \mathbf{u}_z)$ is defined. The z-axis is parallel to the invariance axis of the objects and the position vector **OM** can be written as $\mathbf{OM} = \mathbf{r} + z\mathbf{u}_z$. The scattering system is illuminated by a single source, which radiates a transient field. In particular, we consider a Gaussian pulse shape $F(t)$ whose spectrum is centered at the frequency f_0 and of time duration τ. The expression of this pulse shape is given in equation (1),

$$F(t) \propto \exp\left[-16\frac{(t-\tau)^2}{\tau^2}\right]\sin(2\pi f_0 t). \tag{1}$$

By virtue of the Parseval theorem, solving the scattering problem in the time domain is equivalent to solving it in the frequency domain provided that the fields are replaced by the corresponding time-harmonic ones and the involved frequency range is accurately sampled according to the Nyquist theorem. Therefore, for each frequency f_p, the problem may be expressed by means of the following two coupled integral equations [15], wherein the time factor $\exp(\mathrm{i}\omega_p t)$ has been omitted:

$$E_{\mathrm{s}}^p(\mathbf{r} \in \Gamma) = k_{0,p}^2 \int_\Omega G^p(\mathbf{r}, \mathbf{r}')\chi^p(\mathbf{r}')E^p(\mathbf{r}')\,\mathrm{d}\mathbf{r}', \tag{2}$$

$$E^p(\mathbf{r} \in \Omega) = E_{\mathrm{inc}}^p(\mathbf{r}) + k_{0,p}^2 \int_\Omega G^p(\mathbf{r}, \mathbf{r}')\chi^p(\mathbf{r}')E^p(\mathbf{r}')\,\mathrm{d}\mathbf{r}'. \tag{3}$$

In equations (2) and (3), G^p represents the two-dimensional Green function [15], $k_{0,p}$ is the vacuum wave number for the frequency f_p. The fields E_{inc}, E_{s} and E denote the incident, the scattered and the total fields, respectively. The contrast function $\chi^p(\mathbf{r}) = \varepsilon_c^p(\mathbf{r})/\varepsilon_0 - 1$ relates, at the frequency f_p, the complex equivalent permittivity in Ω, $\varepsilon_c^p(\mathbf{r})$, to that of the host medium. Equation (2) is called the observation equation whereas equation (3) is the field equation. They can be rewritten in a compact form by using symbolic operator notation:

$$E_{\mathrm{s}}^p = \mathbf{K}^p \chi^p E^p, \tag{4}$$

$$E^p = E^p_{\text{inc}} + \mathbf{G}^p \chi^p E^p, \tag{5}$$

where $\mathbf{G}^p : L^2(\Omega) \to L^2(\Omega)$ and $\mathbf{K}^p : L^2(\Omega) \to L^2(\Gamma)$ are the internal and external radiation operators which express, at the operating frequency f_p, the scattered field in Ω and on Γ, respectively.

3. The inversion procedure

The inverse problem aims at finding the contrast function χ such that the transient scattered field measured on Γ, $E_{\text{s}}^{p,\text{mes}}$, matches the scattered field E_{s}^p computed according to equations (4) and (5). To solve this problem, we adopt an inversion strategy which belongs to the class of *bilinear* or *modified gradient* methods [9, 10], where both the contrast and the total field in the investigation domain are considered as unknowns. In this way, one mitigates the overall nonlinearity but increases the number of complex unknowns looked for. In particular, we propose an iterative approach in which, starting from a suitable initial guess, parameters of interest are gradually adjusted by minimizing (for each iteration step) the cost functional:

$$\phi(E, \chi) = W_\Omega \sum_{p=1}^{P} \left\| h_p^{(1)} \right\|_\Omega^2 + W_\Gamma \sum_{p=1}^{P} \left\| h_p^{(2)} \right\|_\Gamma^2, \tag{6}$$

where P denotes the number of frequencies. The residual errors with respect to the state equation (5), $h_p^{(1)}$, and the data equation (4), $h_p^{(2)}$, as well as the normalization terms W_Ω and W_Γ are defined as follows:

$$h_p^{(1)} = E^p - E^p_{\text{inc}} - \mathbf{G}^p \chi^p E^p, \tag{7}$$

$$h_p^{(2)} = E_{\text{s}}^{p,\text{mes}} - \mathbf{K}^p \chi^p E^p, \tag{8}$$

$$W_\Omega = \frac{1}{\sum_{p=1}^{P} \left\| E^p_{\text{inc}} \right\|^2}, \qquad W_\Gamma = \frac{1}{\sum_{p=1}^{P} \left\| E_{\text{s}}^{p,\text{mes}} \right\|^2}. \tag{9}$$

The minimization of the cost functional given in equation (6) is carried out by adopting the M^{2}GM inversion approach [13, 14]; hence the expansion coefficients for the field and contrast function are determined simultaneously. Note that a pixel basis representation is used for both the contrast and the total field. In addition, the contrast function is update along the standard Polak–Ribière conjugate gradient direction of the cost functional; whereas the update direction of the field is properly defined [13, 14]. In order to improve the efficiency of the inversion procedure, we exploit *a priori* information stating that the desired electrical susceptibility must be greater than unity and the conductivity positive. This information is easily introduced in the inversion scheme by expressing the contrast function as:

$$\chi^p = \varepsilon_r - 1 - \mathrm{i}\frac{\sigma}{\omega_p \varepsilon_0} = \xi^2 - \mathrm{i}\frac{\eta^2}{\omega_p \varepsilon_0} \tag{10}$$

where ξ^2 is the electrical susceptibility ($\varepsilon_r = 1 + \xi^2$) and η^2 is the conductivity. These real functions do not depend on the frequency and represent the actual unknowns of the inverse scattering problem. Given the above constraints, the initial guess ($\xi_0 = \eta_0 = 0$) must be rejected since it involves vanishing gradients; indeed, the transformation given in equation (10) introduces a local minima of the cost functional. As a consequence, a different initial guess has to be considered. In the proposed inversion scheme, the back-propagation method has been exploited to provide a suitable initial estimation of the contrast (i.e. ξ_0 and η_0). This value has been used in equation (5) to provide the initial value of the electrical field inside the investigated domain. Mathematical details and additional references on the back-propagation method are given in [17, 18].

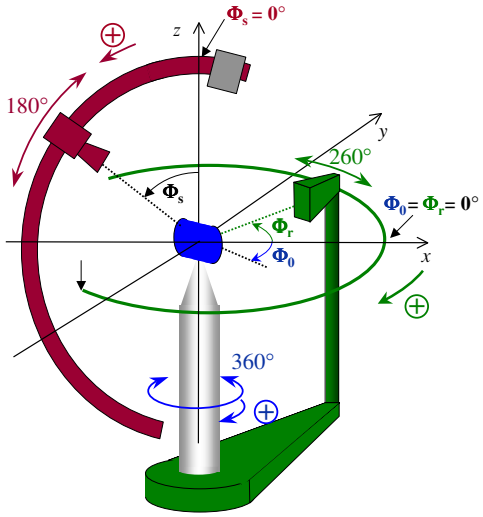

Figure 2. Measurement configuration.

4. The experimental set-up

The reconstruction capabilities of the inversion scheme described in the previous section have been tested against experimental data collected in an anechoic chamber of dimensions $(14 \times 6.5 \times 6.5)$ m^3. The measures have been done by using the arrangement schematized in figure 2, which works with time harmonic fields. The measurement system allows us to consider many locations of the transmitting antenna, which could be turned almost around on a 4 m diameter sphere. In particular, the rotation of the source point is simulated by placing the targets on a rotating plate as sketched in figure 2. Even if multi-view data could be collected, in this paper we consider data measured by illuminating the scattering targets by means of only one source, which is located in ($x = -1.796$ m, $y = 0$ m), with respect to the coordinate system introduced in section 2. The receiver remains in the azimuthal plane $(O, \mathbf{u}_x, \mathbf{u}_y)$ and, for practical reasons, its excursion is restricted to the angular range $-130^\circ \leqslant \Theta_r \leqslant 130^\circ$ on a circumference whose radius is 1.795 m. The position of the receiver is shifted with an angular step $\Delta\Theta_r = 1^\circ$, so that the incident field, i.e. the field measured without any object, and the total field, i.e. the field in the presence of the target, are measured in $N_m = 261$ different points. Therefore, the time harmonic scattered field is obtained by subtracting the incident field from the total one. The measurements were acquired by means of a vector network analyzer (Agilent-HP 8510) and by using wide-band ridged horn antennas (ARA DRG 118) as transmitter and receiver. The measurements are performed with 792 frequencies uniformly distributed from 1 up to 18 GHz. The electrical field is vertically polarized along the z-axis in the azimuthal plane $(O, \mathbf{u}_x, \mathbf{u}_y)$. The considered objects are shown in figure 3. Both of them are inhomogeneous and have a length equal to 1.5 m; hence they are long enough to allow a two-dimensional assumption. The first scatterer, figure 3(a), consists of two dielectric cylinders with the circular cross section located one inside the other one (FoamDielInt) [16]. The larger cylinder is made by polyurethane foam (SBF300) and has a diameter of 0.08 m; the smaller one is of plastic (berylon) and its diameter is equal to 0.03 m. The dielectric constants of these plastics were measured by means of the commercial kit EpsiMu [19] and were found to

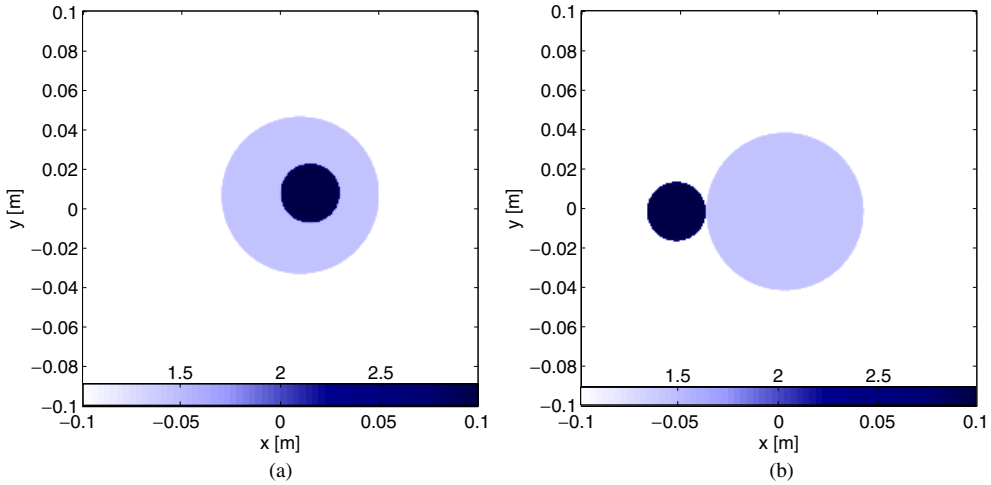

Figure 3. Targets under test. (a) FoamDielInt object, (b) FoamDielExt object.

be almost constant into the considered frequency range (1–18 GHz). The measured values of the relative permittivity are $\varepsilon_r = 1.45$ for foam and $\varepsilon_r = 3.0$ for berylon; their conductivities are negligible. The second scatterer is made by the same two dielectric cylinders but in this case the smaller one is outside and close to the larger one, as shown in figure 3(b).

5. Choice of non-redundant amounts of data

The adopted experimental setup employs many receivers, which measure the electromagnetic fields in a wide frequency range, which is densely sampled; hence, a huge amount of data are provided. On the other hand, the question arises about the usefulness of all these data, or in other words if the available information is redundant or it is effectively necessary to improve the reconstruction capability of the imaging strategy. In order to give an answer to this question, it is worth recalling that the properties of the scattered field (i.e. the data of the inversion procedure) can be deduced from those of the radiation operator **K**. As shown in [20], with respect to large scatterers (as compared with the wavelength) and typical measurement setups, in which both primary sources and measurement probes are placed at some wavelength apart from the object under test, the scattered field can be represented, within a given accuracy, with a finite number of parameters. This number depends only on the electrical size of the scatterer and represents the essential dimension of the space of the data. Moreover, as discussed in [21, 22] the amount of non-redundant information can be increased if the transmitting and receiving probes are located in close proximity to the scatterer and if they can work in a multi-frequency mode. As shown in [23], by virtue of the compactness of the radiation operator **K**, the properties of the field radiated from an arbitrary source can be inferred through the singular value decomposition (SVD) of **K**. Therefore, let $\{u_n, \sigma_n, v_n\}$ denote the singular system of **K**, σ_n being its singular value and u_n and v_n the right- and left-hand singular functions, respectively; the amount of independent data can be easily evaluated by plotting the singular values σ_n which are higher than a threshold, whose value depends on the noise affecting the data, i.e. on the measures accuracy [21]. By taking into account the above statements, we are able to evaluate numbers of receivers and frequencies, which

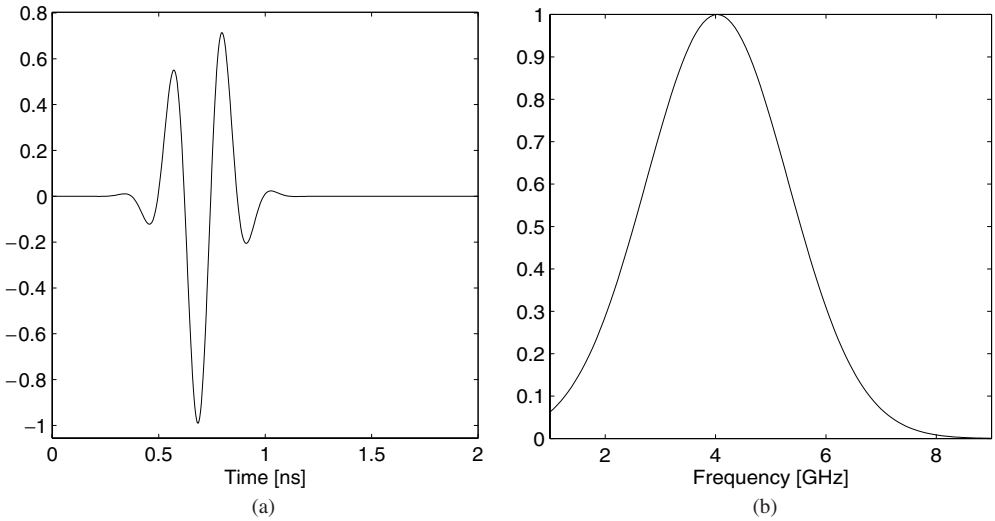

Figure 4. Pulse shape of the incident field. (a) In the time domain, (b) modulus of its Fourier transform.

are required to collect all available independent information. Let us consider the particular case in which a Gaussian incident pulse shape defined according to equation (1) is assumed as an incident field. In particular, we limit our analysis to an incident pulse whose spectrum is centered at $f_0 = 4$ GHz and of time duration $\tau = 0.7$ ns. This pulse and its spectrum are shown in figure 4. Under these hypotheses, the operator **K** has been defined in the frequency range 2–7 GHz, i.e. at those frequencies where the spectrum of the incident field is not negligible, and on a square domain of side size 0.2 m. This last one is the investigating domain assumed to test the inversion strategy and it is larger than the minimum circle enclosing the scatterers [21]. As a consequence, the SVD of **K** provides an upper bound of the essential dimension of the space of data. As far as the number of frequencies is concerned, it is worth noting that the Nyquist theorem has to be respected in order to ensure that solving the inverse problem in the frequency domain is equivalent to solving it in the time domain. By taking into account the distance between the source point and the receiving probe fixed in the experimental device ($\Delta R \approx 3.6$ m) and assuming a wave velocity at least equal to that of free space c_0, we have estimated that a time longer than 12 ns is required to measure the scattered field. As a consequence, we have fixed the frequency step equal to $\delta f = 64.5$ MHz.[3] On the other hand, to estimate the number of required receivers, terms u_n, σ_n, v_n have been evaluated using a standard numerical procedure and by changing the number of receivers, which are uniformly spaced on the measurement line. The behavior of singular values is plotted in figure 5. Since the use of more than 27 receivers does not increase the number of significant singular values (i.e., those larger than the chosen threshold -20 dB[4]), one may conclude that $N_m = 27$ receivers uniformly spaced in angle on the measurement line Γ are sufficient to collect all the independent data.

[3] This step is sufficiently dense to ensure that all the independent data provided by the frequency diversity are taken into account. This may be proved by observing the behavior of the singular value of **K**.

[4] This value has been fixed by considering the measurement accuracy provided by the experimental setup.

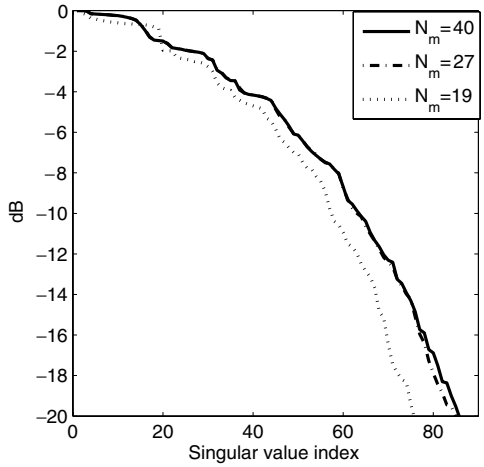

Figure 5. Behavior of the singular values.

6. Inversion results

This section aims at testing the proposed inversion approach against data collected by means of the experimental setup presented in section 5.

Measurements were carried out in the frequency domain; hence the transient scattered field, which is the datum of the imaging strategy, is determined by weighting the measured scattered field by the spectrum of a chosen pulse shape and by carrying out the inverse temporal Fourier transform. The reconstruction procedure also requires knowledge of the transient incident field into the investigating domain Ω. This field has been obtained by means of a two-step procedure. In order to take into account the radiation pattern of the transmitting antenna used in the experimental setup, the first step aims at properly weighting the field radiated in the domain Ω by a line source. The complex weighting coefficient γ for a single frequency has been evaluated by imposing the equality:

$$E_{\text{inc}}^{\text{mes}}(\mathbf{r}_m) = \gamma E_{\text{inc}}^{\text{theo}}(\mathbf{r}_m), \qquad \mathbf{r} \in \Gamma, \tag{11}$$

where $E_{\text{inc}}^{\text{mes}}$ is the measured incident field on the surface Γ, $E_{\text{inc}}^{\text{theo}}$ is the field radiated on Γ by a line source with unitary current, and $\mathbf{r}_m$ denotes the opposite position to that of the transmitting antenna, i.e. $x_m = 1.796$ m and $y_m = 0$ m. The second step provides the transient incident field in Ω from the time-harmonic components of the field by applying the same operations described above with reference to the scattered field.

Since the transient scattered field on Γ as well as the incident field in Ω are synthesized from time-harmonic fields, we may test the effectiveness of the inversion strategy by using different incident pulse shapes. Limiting our attention to Gaussian incident pulses equation (1), we have initially considered a pulse whose spectrum has a central frequency $f_0 = 2$ GHz and having a time duration of $\tau = 2$ ns. The spectrum of this pulse is plotted in figure 6(a). Figure 7 shows the reconstructed permittivity profiles related to the FoamDielInt and FoamDielExt, respectively. These reconstructed profiles are to be compared to actual profiles plotted in figure 3. These pictures show that a quite satisfactory reconstruction is obtained in the case of the FoamDielInt object, but not for the FoamDielExt target. Indeed, the berylon cylinder is only localized and not correctly characterized. The resolution could be improved by using a central-frequency hopping approach [24]. However, this approach

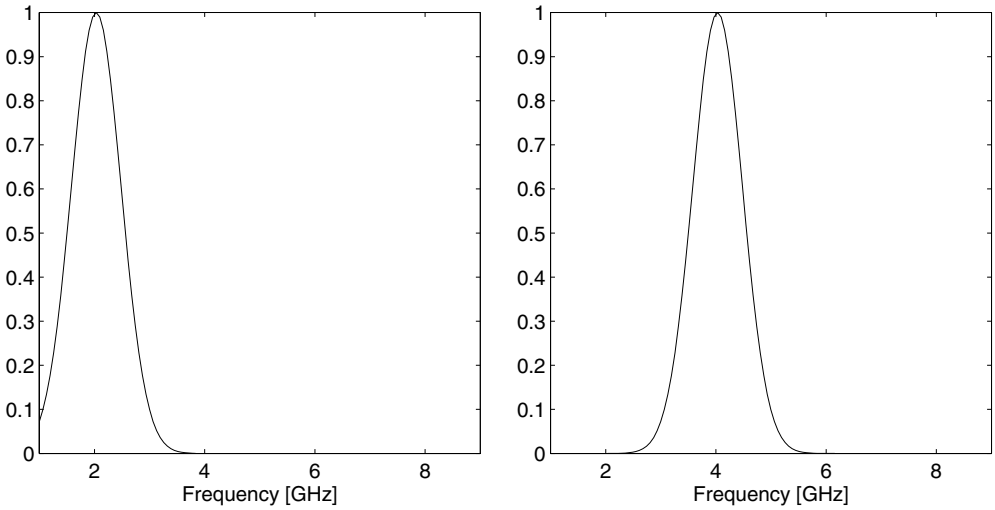

Figure 6. Incident pulse shapes. (a) $f_0 = 2$ GHz, $\tau = 2$ ns; (b) $f_0 = 4$ GHz, $\tau = 2$ ns.

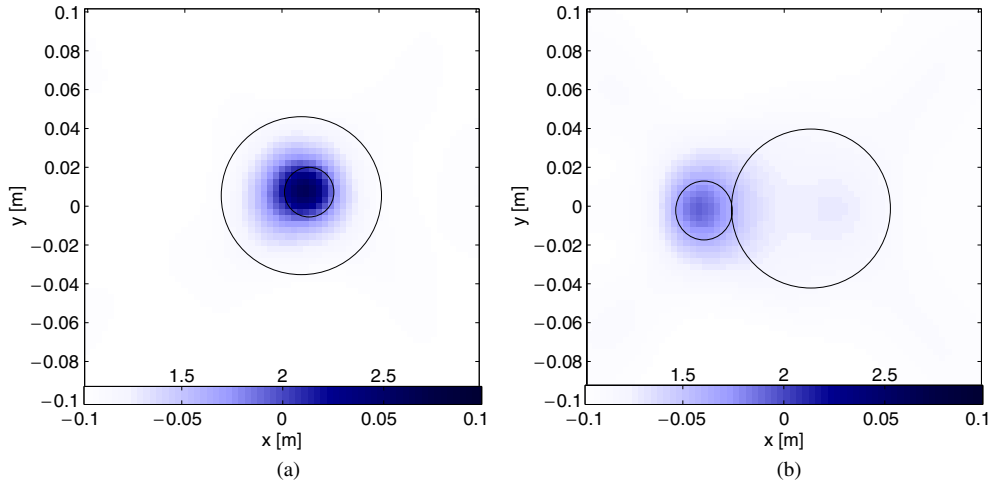

Figure 7. Reconstructed permittivity profile using the Gaussian incident pulse having a central frequency $f_0 = 2$ GHz and time duration $\tau = 2$ ns: (a) FoamDielInt (b) FoamDielExt.

requires targets under test to be illuminated successively with different incident fields having spectra centered at increasing frequencies. The initial guess for the inversion, related to an illumination, is the final result obtained using a pulse with a lower central-frequency. In the present paper, we investigate the improvement of the resolution using a single source. We have then shifted the central frequency f_0 from 2 GHz up to 4 GHz, keeping unchanged the choice of the initial guess (the one deduced with the back-propagation procedure). The spectrum of this pulse is plotted in figure 6(b). By doing so, the inversion procedure is no longer able to retrieve correctly the FoamDielInt object; the reconstructed permittivity profile

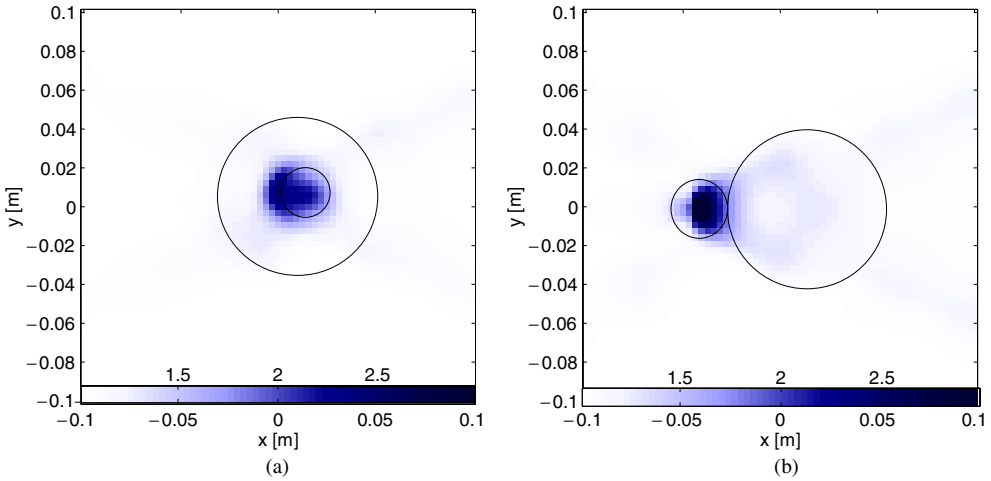

Figure 8. Reconstructed permittivity profile using the Gaussian incident pulse having a central frequency $f_0 = 4$ GHz and time duration $\tau = 2$ ns: (a) FoamDielInt, (b) FoamDielExt.

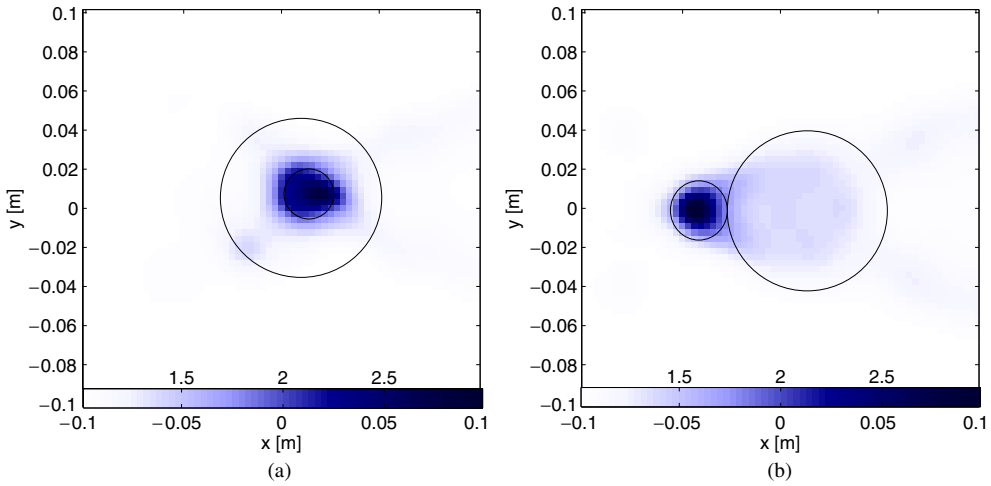

Figure 9. Reconstructed permittivity profile using the Gaussian incident pulse having a central frequency $f_0 = 4$ GHz and time duration $\tau = 0.7$ ns: (a) FoamDielInt; (b) FoamDielExt.

is given in figure 8(a). On the other hand, not negligible improvements are obtained with respect to the FoamDielExt, as shown in figure 8(b). These results can be explained by taking into account that increasing the frequency not only the resolution power but also the degree of nonlinearity increases [25]. Therefore, the probability to obtain a false solution, i.e. the minimization process is trapped into a local minima, is enhanced. As a consequence of the above considerations, an incident pulse with spectrum centred at $f_0 = 4$ GHz and of time duration $\tau = 0.7$ ns has been taken into account; the pulse and its spectrum are given in figure 4. Since the time duration of the impulse has been reduced its spectrum is significantly larger than the previous ones. In this way, both low and high frequencies are exploited at

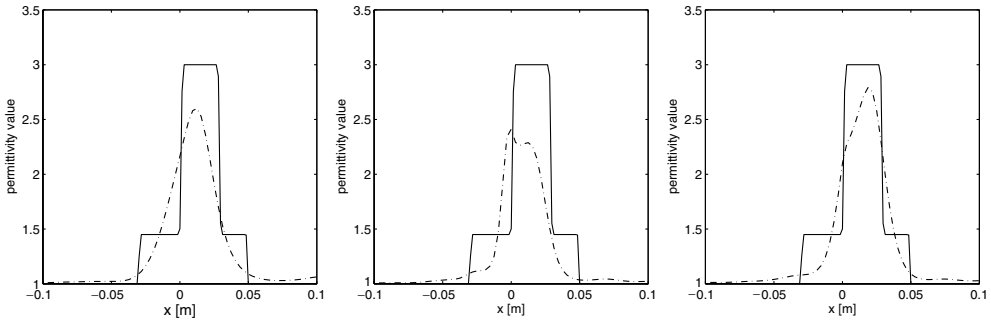

Figure 10. Comparisons between the reconstructed profile and the actual one along the illumination direction for the target FoamDielInt for different choices of incident pulse. (a) $f_0 = 2$ GHz and time duration $\tau = 2$ ns, which corresponds to the reconstruction presented in figure 7(a); (b) $f_0 = 4$ GHz and time duration $\tau = 2$ ns, which corresponds to the reconstruction presented in figure 8(a); (c) $f_0 = 4$ GHz and time duration $\tau = 0.7$ ns, which corresponds to the reconstruction presented in figure 9(a).

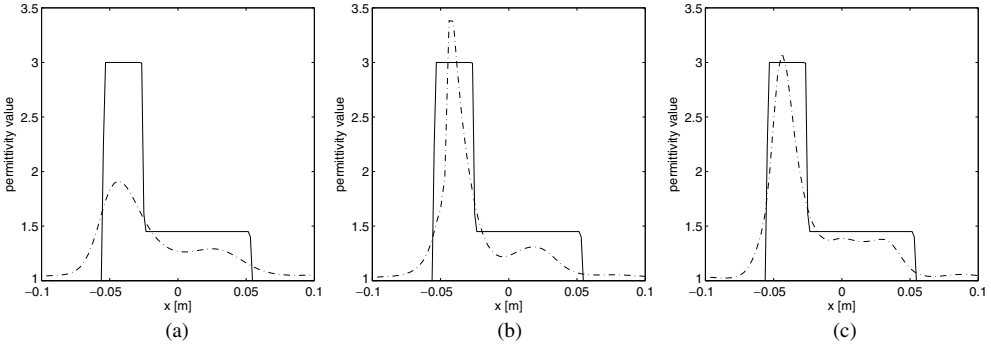

Figure 11. Comparisons between the reconstructed profile and the actual one along the illumination direction for the target FoamDielExt for different choices of incident pulse. (a) $f_0 = 2$ GHz and time duration $\tau = 2$ ns, which corresponds to the reconstruction presented in figure 7(b); (b) $f_0 = 4$ GHz and time duration $\tau = 2$ ns, which corresponds to the reconstruction presented in figure 8(b); (c) $f_0 = 4$ GHz and time duration $\tau = 0.7$ ns, which corresponds to the reconstruction presented in figure 9(b).

the same time, then one may preserve the robustness of the inversion approach against local minima while increasing its resolution power. Therefore, a positive effect on the performances of the inversion procedure is achieved, as one can state by observing the reconstructed profiles plotted in figure 9, where both targets FoamDielInt and FoamDielExt are accuratlly retreived. To emphasize improvements offered by the use of a large spectrum incident pulse, quantitative comparisons between the reconstructed profiles and the actual ones along the direction of the illumination are given in figures 10 and 11.

Finally, it is worth remarking that only the reconstructed permittivity profiles have been shown because in all cases a negligible conductivity has been retrieved. This agrees with the dielectric nature of the scatterers. Moreover, all the proposed results have been obtained by discretizing the investigating domain Ω into 64×64 square cells and by considering only 30 iteration steps. Such a number has been sufficient to achieve the convergence of the

minimization process. We did not observe any marked changes by continuing the iterative process.

7. Conclusion

In this paper, the problem of reconstructing the electromagnetic parameters of dielectric cylindrical targets from a single-view transient scattered field has been addressed. By taking advantage of the Parseval theorem the problem has been tackled in the frequency domain and an iterative inversion approach based on the M^2MG method has been proposed. The effectiveness of this strategy has been enhanced by exploiting the *a priori* information that the materials, which are usually involved into non-invasive diagnostic applications, are characterized by an electrical susceptibility greater than unity and a positive conductivity. The reconstruction capabilities of the inversion strategy have been tested against experimental data collected by means of an experimental setup which works with time harmonic fields. This allows us to adopt different incident pulse shapes, even if in this paper we have limited our attention to Gaussian ones. In particular, we have investigated how the achievable performances may depend on the time duration of the incident pulse and/or the central frequency of its spectrum. The results presented in this paper show that the robustness of the inversion procedure against local minima and its resolution power can be improved by illuminating the targets with a single pulse having a large spectrum. These results encourage to apply the proposed approach to investigate complex scenarios such as, for instance, the case of an inhomogeneous background characterized by none constant electromagnetic parameters. Moreover, the use of two or more illumination views appears also interesting to investigate in order to further improve the accuracy of the inversion strategy.

References

[1] Devaney A J 1984 Geophysical diffraction tomography *IEEE Trans. Geosci. Remote Sens.* **22** 3–13
[2] Bolomey J C 1989 Recent European developments in active microwave imaging for industrial, scientist and medical applications *IEEE Trans. Theory Tech.* **37** 2109–17
[3] Miller E L, Klimer M and Rappaport C 2000 A new shape-based method for object localization and characterization from scattered field data *IEEE Trans. Geosci. Remote Sens.* **38** 1682–96
[4] Colton D and Kress R 1992 *Inverse Acoustic and Electromagnetic Scattering Theory* (Berlin: Springer)
[5] Bertero M and Boccacci P 1998 *Introduction to Inverse Problems in Imaging* (Bristol: Institute of Physics Publishing)
[6] Belkebir K and Saillard M 2001 Special section: testing inversion algorithms against experimental data *Inverse Problem* **17** 1565–71
[7] Belkebir K and Saillard M 2005 Special section on testing inversion algorithms against experimental data: inhomogeneous targets *Inverse Problem* **21** S1–3
[8] Brancaccio A, Pascazio V and Pierri R 1995 A quadratic model for inverse profiling: the one dimensional case *J. Electromagn. Waves Appl.* **9** 673–96
[9] Kleinman R E and van den Berg P M 1993 An extended range-modified gradient technique for profile inversion *Radio Sci.* **28** 877–84
[10] Isernia T, Pascazio V and Pierri R 1997 A non linear estimation method in tomographic imaging *IEEE Trans. Geosci. Remote Sens.* **35** 910–23
[11] Ligthart L P, Yarovoy A G and Kirana A Y 2003 Gpr antenna simulation and optimization in time domain *Proc. 4th Int. Conf. on Antenna Theory and Tech. vol 1* pp 21–4
[12] Kleinman R E and van den Berg P M 1992 A modified gradient method for two-dimensional problems in tomography *J. Comput. Appl. Math.* **42** 17–35
[13] Belkebir K and Tijhuis A G 2001 Modified^2 gradient method and modified Born method for solving a two-dimensional inverse scattering problem *Inverse Problem* **17** 1671–88
[14] Dubois A, Belkebir M and Saillard K 2005 Retrieval of inhomogeneous targets from experimental frequency diversity data *Inverse Problem* **21** S69–79

[15] Chew C W 1995 *Waves and Fields in Inhomogeneous Media* (Piscataway, NJ: IEEE)
[16] Geffrin J-M, Sabouroux P and Eyraud C 2005 Free space experimental scattering database continuation: experimental set-up and measurement precision *Inverse Problems* **21** S117–30
[17] Kleinman R E and van den Berg P M 1994 Two-dimensional location and shape reconstruction *Radio Sci.* **29** 1157–69
[18] Belkebir K, Bonnard S, Pezin F, Sabouroux P and Saillard M 2000 Validation of 2D inverse scattering algorithms from multi-frequency experimental data *J. Electromagn. Waves Appl.* **14** 1637–67
[19] Sabouroux P and Bosci P 2005 Epsimu: a new microwave materails measurement kit *Rev. Electr. Electron.* **10** 58–63
[20] Bucci O M and Franceschetti G 1989 On the degree of freedom of scattered field *IEEE Trans. Antennas Propag.* **37** 918–26
[21] Bucci O M, Crocco L and Isernia T 1999 Improving the reconstruction capabilities in inverse scattering problems by exploiting 'near proximity' *J. Opt. Soc. Am.* A **16** 1788–98
[22] Bucci O M, Crocco L, Isernia T and Pascazio V 2001 Subsurface inverse scattering problems: quantifying, qualifiying and achieving the available information *IEEE Trans. Geosci. Remote Sens.* **39** 2527–38
[23] Bucci O M and Isernia T 1997 Electromagnetic inverse scattering retrievable information and measurement strategies *Radio Sci.* **32** 2123–38
[24] Dubois A, Geffrin J M, Belkebir K and Saillard M 2006 Imaging of dielectric cylinders from experimental stepped-frequency data *Appl. Phys. Lett.* **88** 164104
[25] Bucci O M, Cardace N, Crocco L, Isernia T and Pascazio V 2001 Degree of non-linearity and a new solution procedure in scalar 2-d inverse scattering problems *J. Opt. Soc. Am.* A **18** 1832–45